

Green Synthesis of Uracil Derivatives, DNA Binding Study and Docking-based Evaluation of their Anti-cancer and Anti-viral Potencies

Vadivelan Rengasamy¹, Mohd Suhail^{2*} and Arvind Jain¹

¹Department of Chemistry, School of Basic and Applied Sciences, Galgotias University UP, India

²Department of Chemistry, Jamia Millia Islamia, (A Central University) New Delhi, India

***Corresponding Author:** Mohd Suhail, Department of Chemistry, Jamia Millia Islamia, (A Central University) New Delhi, India.

Received: November 22, 2021

Published: December 22, 2021

© All rights are reserved by , Mohd Suhail, et al.

Abstract

In the last few decades, the world has faced a lot of major diseases such as cancer, AIDS and COVID-19. With the advent of disease, different medicines were also worked on but not every medicine could work against more than one major disease. Thus, the world needs such medicine that could act alone against different diseases with different mechanisms at the same time. In this condition, uracil derivatives also known as nucleoside derivatives came as a ray of hope, and have played an important role to cure many diseases. Hence, new twelve uracil derivatives were synthesized by a highly efficient one-pot inexpensive method successfully. It is fully confirmed that one-pot synthesis not only produces a maximum yield of products but also gives insights into green chemistry due to the reduction in byproducts, waste, energy and cost. Moreover, as per literature data, uracil derivatives (i) bind with DNA in the cancer-curing step, and (ii) interrupt the replication process of the virus during antiviral activity. Hence, DNA binding study was also done experimentally, whose results suggest that the reported compounds bind to DNA through intercalation modes. Only three out of twelve drugs were found to have a greater affinity towards DNA, which were selected for the docking study so that the binding pockets of DNA for the selected drugs, can be evaluated. The docking results exposed the formation of DNA-compound adduct. Furthermore, by following the same docking method, the interactions taking place between newly synthesized uracil derivatives and their literature data-based target, were studied. It revealed that newly synthesized drugs may also exhibit antiviral activity.

Keywords: Uracil Derivatives; DNA Binding Study; Docking Study; Anti-cancer; Antiviral

Introduction

Diseases are common to us. Some diseases such as cancer and AIDS have engulfed the world. These diseases are very dangerous and have become the leading cause of death in developed and under developed countries. In the same way, COVID-19 has also stood up in front of the world, and made its place inside the world. In this condition, the world needs a single medicine that can act alone against different major diseases. Although several drugs have been synthesized for the treatment of such fatal diseases, the drug that has attracted the scientists of the entire world, is uracil derivatives which have shown tremendous effect against not only cancer [1-

8] but also viruses such as HIV [9-11], hepatitis B and C [12,13], the herpes viruses [14], and so forth. As per literature data [10,11], uracil derivatives can be classified as nucleoside reverse transcriptase inhibitors that interrupt the main function of the reverse transcriptase (RTs) enzyme of HIV. Actually, uracil derivatives block the action of viral reverse transcriptase enzyme, which is necessary for HIV to replicate. Besides, uracil derivatives have also shown their versatility by acting against SARS-CoV-2 [15-17]. Hence, the importance of such drugs can not be ignored in the current pandemic situation. Like uracil derivatives, there are several nucleotide analog drugs, including remdesivir, favipiravir, ribavirin, galidesivir, and

EIDD-2801. These drugs efficiently inhibit SARS-CoV-2 replication [18]. 5-Fluorouracil or 5-chlorouracil were the first pharmacologically active uracil derivatives [1-8]. Although 5-fluorouracil is available for the treatment of cancer, we are not fully equipped with drugs that can treat cancer effectively at late stages and without demonstrating any side effects [19,20]. The presently available anticancer drugs show serious side effects, e.g., poor solubilities, narrow therapeutic windows and intensive cytotoxicities to normal tissues [21]. Besides, some anticancer drugs have solubility and bioavailability issues; making them less effective [21,22]. Therefore, the search for new agents for the treatment of different major diseases is an urgent need today.

The versatility of uracil derivatives has made them privileged structures. Their antioxidant property [23] has made them an anticancer agent. Recently, chemists paid more attention to uracil analogs, some pharmacologically important analogs are shown in figure 1. In the development of derivatives possessing better pharmacological and pharmacokinetic properties (increased bioactivity, selectivity, metabolic stability, absorption, and lower toxicity) many modifications of uracil have been performed so far to tackle toxicity problems. Uracil and its derivatives are the important key starting material for the preparation of many organic molecules, drug substances and drug intermediates [24,25]. Tegafur-uracil is a chemotherapy drug used in the treatment of cancer, primarily bowel cancer [26]. Thus, the synthesis of new uracil derivatives is an important and useful task in organic chemistry. In recent years, the synthesis of uracil derivatives has been reported. By keeping literature-based facts into consideration, efforts were made to discover a new environment-friendly protocol for the synthesis of uracil derivatives. This protocol involved one-pot and one solvent with low cost. It is because one-pot synthesis not only produces a maximum yield of products but also gives insights into green chemistry [27]. Besides, green chemistry approaches are significant due to the reduction in byproducts, waste, energy and cost [27]. The possibility of performing multistep reactions under one-pot synthesis could enhance their efficiency from an economic as well as an ecological point of view.

As per literature data, uracil derivatives interact with DNA during the cancer-curing step [8,28,29]. It is because DNA is the pharmacological target of many anticancer drugs that are currently in clinical use or advanced clinical trials. Besides, cell functions (transcription and replication) can be regulated by targeting DNA. It all seems logical, intuitively appealing, and conceptually straightforward. The small ligand molecules act as a drug when alteration or

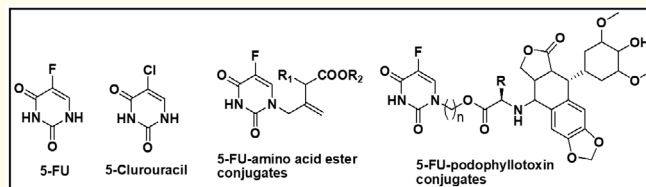


Figure 1: Some pharmacologically important uracil derivatives.

inhibition of DNA function is required to cure or control the disease [30]. Therefore, the study of the interaction of the newly synthesized compounds with DNA was very exciting and significant not only to access their biological potential but also in understanding the mechanism of interaction. UV-vis. spectroscopy is perhaps the simplest and most commonly used method for the investigation of the stability of DNA and its interactions with small ligand molecules [31]. The study of interactions could be notified by monitoring the changes in the absorption properties of the drug or the DNA molecules. Besides, the comparative study of the position of absorption bands of free DNA and drug bounded DNA, indicates an interaction between the DNA and the ligand molecules [32-36].

Another most important thing to be kept in the mind was the inhibition of replication of HIV by uracil derivatives, which they do by means of interfering in the main function of reverse transcriptase (RTs) enzyme [10,11]. Hence, keeping the facts described above into consideration, one-pot synthesis of uracil derivatives was done successfully. Besides, in the docking study, DNA as well as RTs, were selected as the target for newly synthesized uracil derivatives.

Experimental section

Material and methods

All the reagents and chemicals were obtained from the highest grade available from Sigma Aldrich, Acros organics, Spectrochem, Loba Chem, Survival Technology and Rankem Laboratories, and were used without purification. TLC was performed on Merck TLC Silica gel 60 F254 plates eluting with specific solvents and samples were made visual with a UV lamp, Silica gel (60-120 mesh) was used for column chromatography. Melting points were measured with an Electrothermal 9100 apparatus. High-resolution mass spectra were recorded on Bruker spectrometer. The measurement was run in positive ion mode. ¹H-NMR was obtained using Bruker (400 MHz) spectrometer in DMSO and CDCl₃ with tetramethylsilane as an internal standard. Chemical shifts are reported in parts

per million (δ), coupling constants (J values) are reported in hertz (Hz) and spin multiplicities are indicated by s (singlet), d (doublet), t (triplet), q (quartet), m (multiplet).

Synthesis of compounds 1-4

Synthesis of N-alkylated compounds of 6-chlorouracil (1)

Charged 6-chlorouracil (10.0g, 0.06 M) and diisopropylethylamine (18.52g, 0.14 M) were dissolved in 50 mL DMF and the mixture was stirred for 10 min at room temperature then halogenated 1-(bromomethyl)benzene (0.06 M) was added to the reaction mixture and stirring was continued for 8 hrs at room temperature. After completion of the reaction, 150 mL water was added into the mixture and the precipitated product 1 was filtered, dried and obtained 14.37g, 89% yield.

Synthesis of compound (2)

Compound 1 (10.0 g, 0.04 M) was dissolved in 100 ml acetone followed by potassium carbonate (12.84g, 0.09 M) and the reaction mass was stirred for 15 min at room temperature, then methyl iodide (11.99 g, 0.08 M) was added and left the reaction mass at stirring overnight. After completion of the reaction, water was added to the mixture and the precipitated product (2) was collected by filtration method, dried and obtained 9.74 g, 92.0% yield.

Synthesis of Compound 3 or 4

Charged compound 2 (9.0 g, 0.03 M) was dissolved in 45 mL DMF followed by the addition of potassium carbonate (9.25 g, 0.06 M). Then piperazine (3.60 g, 0.04 M) or piperidine-3-amine (6.83 g, 0.039 M) was added, and the reaction mixture was heated at 80°C. After the completion of the reaction, the mixture was cooled to room temperature by the addition of water slowly. After that dichloromethane was used for the extraction. The organic layer was separated and dried over sodium sulphate. Finally, the solvent was removed under reduced pressure for the formation of compounds 3 (9.16, 85%) or 4 (9.81 g, 87%).

One-pot synthesis of target compounds (A-L)

Charged 6-chlorouracil (7.75 g, 0.05M) and potassium carbonate (9.14 g, 0.06 M) were dissolved in 50 mL DMF in 250 mL RBF, followed by the halogenation using 1-(bromomethyl) benzene (10 g, 0.05M). The reaction mixture was stirred for 8 hrs at room temperature. Then, methyl iodide (15.02 g, 0.10 M) and potassium carbonate (7.31 g, 0.0529 M) were added to the reaction mixture and stirring was extended overnight at the same temperature. After that, the charged piperidin-3-amine (9.10 g, 0.05 M) or piperazine

(4.52 g, 0.05 M) was added to the reaction mixture and heated at 80 °C for 8hrs to obtain charged compound 3 or 4. Finally, the (S)-2-((methoxycarbonyl)amino-3-methylbutanoic acid (9.22g, 0.05 M) i.e. Moc-L-Valine was added to the reaction mixture in the presence of coupling reagent HATU (40.23 g, 0.10 M) and triethylamine (10.71 g, 0.10M) and the reaction mixture was stirred for 20 min at room temperature. After the completion of the reaction, water was added and the product was extracted in ethyl acetate, an organic layer that was dried over sodium sulphate. After that, the solvent was removed under reduced pressure. The desired products were purified by column chromatography to get title compounds (A-L).

Charged compound 3 (9.0 g, 0.02 M) or 4 (9.0 g, 0.028 M) was initially dissolved in 90 mL dichloromethane, after the addition of HATU (16.12 gm, 0.0423 moles) followed by Moc-L-Valine (5.20 gm, 0.02968 moles), TEA (5.72 gm, 0.0565 moles) was added, and the reaction mass was stirred at room temperature till the completion of the reaction. The organic layer obtained after the addition of water, was dried with sodium sulphate. Finally, the title compounds were obtained by removing the solvent under reduced pressure.

Chemistry

The synthesis of the target uracil derivatives was performed according to Scheme 1 (Figure 2). A simple and successful protocol has been developed for the synthesis of uracil derivatives. According to literature data, generally in benzylation and methylation reactions, bases like sodium hydride in dimethylformamide have been used which is highly dangerous in the context of safety and environmental pollution. Besides, it also results in poor yield and impure compounds. It was observed that the reaction was completed at a faster rate, but less conversion was observed when an organic base was used. On the other hand, the percentage of yield was increased when the inorganic base was used. Hence, throughout the reactions in our simple protocol, we used a low-cost, ecofriendly and safe inorganic base potassium carbonate in dimethylformamide solvent in one pot during four steps which is one of the major advantages of our protocol. In addition, we got higher percentage yields of products. Initially, we synthesized N-substituted uracil analogs in high yields by simple N-benylation and N-methylation of 6-chlorouracil with benzyl halides and methyl iodide respectively, under catalyst-free conditions in DMF solvent. After that, the chlorine atom of N-substituted uracil derivatives was substituted with piperazine or 3-aminopiperidine. In the last step, with similar conditions and solvent, amino acid coupling reactions were done in the presence of coupling reagent HATU (1-bis(dimethylamino)

methylene-1H-1,2,3-triazolo [4,5-b]pyridinium-3-oxid hexafluorophosphate) for the formation of target compounds A-L. The whole synthesis was done with one solvent in one pot that results in the reduction of industrial waste, effluent generation and overall good yields (49-60%) of final products. A reasonable mechanism for the formation of uracil derivatives is shown in Scheme 2 (Figure 3).

Figure 2: Scheme 1 for the novel synthesis of uracil derivatives.

Reagents and conditions: (a) K₂CO₃/DMF, Stirring, R.T, 8 hrs
(b) K₂CO₃/DMF, CH₃I, R.T, 24 hrs (c) K₂CO₃/DMF/
3-aminopiperidine, heat, 80 °C, 8 hrs (d) K₂CO₃/DMF/
Piperazine, heat, 80 °C, 8 hrs (e) HATU, TEA, Moc-L-Valine/
DMF, R.T, 20 min.

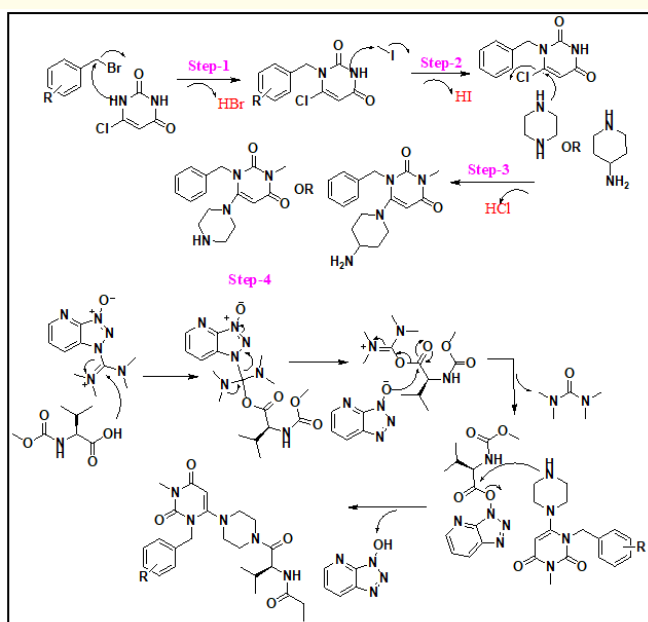


Figure 3: Proposed mechanism for the synthesis of uracil derivatives.

DNA binding study

For DNA binding study, absorption titration experiments were performed with fixed concentrations of the compounds. The compounds were dissolved in a mixture of 1% DMSO and 99% Tris-HCl buffer (10⁻² M, pH 7.4). Stock solutions of newly synthesized compounds, as well as calf-thymus DNA (Ct-DNA), were prepared, stored at 4 °C, and used after no more than one week. Initially, a UV absorption spectrum of Ct-DNA in buffer solution was recorded that showed two absorption bands at 230 nm and 260 nm with absorbance ratio = 1.8, which indicated the free nature of DNA [37]. UV absorbance at 260 nm after 1: 40 dilutions with a known molar absorption coefficient value of 6600 M⁻¹ cm⁻¹ determined the concentration of DNA. Absorption titration experiments were performed in the absence and presence of different concentrations (0.2 – 1.4 × 10⁻³) of Ct-DNA. The intrinsic binding constant (K_b) was determined with help of Eq. 1, which was initially known as Benesi-Hilderbrand equation and then modified by Wolfe., *et al.* [38].

$$\dots\dots\dots (1)$$

Where, absorption coefficients, ϵ_a , ϵ_f , and ϵ_b correspond to A_{obs}/[compound], extinction coefficient for the compound and the extinction coefficient for the compound in the fully bound form, respectively. The binding constants for the different compounds (K_b) were determined by the slopes and the intercepts of the plots of .

$$\frac{[DNA]}{(\epsilon_a - \epsilon_f)} \text{ vs } [DNA]$$

Docking study

To predict the interactions of newly synthesized drugs with various macromolecules at the supramolecular level, molecular docking is a useful tool. In this section, we have described the various interactions of newly synthesized drugs with DNA as well as the reverse transcriptase enzyme. To predict the mode of binding with DNA, only three target compounds (F, G and H) were selected because of their high experimental DNA binding affinity. On the other hand, all target compounds were selected to predict the mode of binding with RTs.

The software used in the docking study was MarvinSketch, Autodock tool [39], Discovery studio, Autodock vina [40], PyMOL and LigPlot [41]. The crystalline structure of DNA [42] and the reverse transcriptase enzyme of HIV [43] with pdb codes 1bna and 2rf2, respectively were obtained from the protein data bank [https://www.rcsb.org/]. The currently presented docking study

involved the following steps.

Receptor purification and preparation

The crystalline structures of the receptors obtained from the protein data bank, were made pure for the docking purpose using discovery studio (Figure 4). There were many unwanted things to be removed that were associated with the main receptors (RTs and

Figure 4: The crystalline structure of computationally cleaned receptors for newly synthesized drugs.

DNA) such as undesirable residues, water molecules, and other non-required ligands.

Ligand preparation

Having prepared the receptor file, the structures of ligands

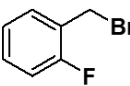
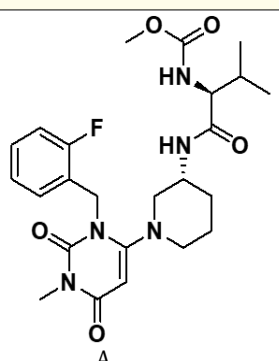
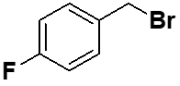
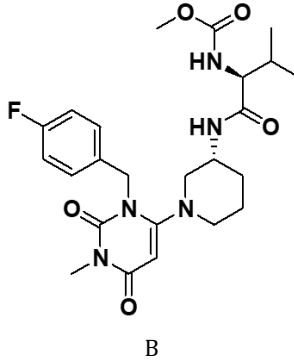
(newly synthesized drugs) were drawn using MarvinSketch. After that, the confirmation of the 3D structure of the ligands was done with the help of Discovery studio.

Docking and data analysis

After the preparation of the receptors and ligands, both were docked using the Autodock tool, and then binding affinities were observed using Autodock vina. PyMOL was used to find out the total number of hydrogen bonds and the residues involved in it, while the LigPlot was used to find out hydrophobic interactions between the receptor and ligands.

Results

The proposed structures of A-L were well supported by analytical and spectroscopic data. The compounds A-L were found as solids with good yields, stable to air, and quite soluble in ethylacetate, methanol, ethanol, DMSO, DMF. The characteristic signal from the CH_3N - group in the ^1H NMR spectrum was observed as a singlet at ~ 2.90 - 3.10 ppm, alkenic proton of uracil ring CH - was observed at 5.00 - 5.35 ppm, benzylic proton $-\text{CH}$ at 4.86 - 5.37 ppm, aromatic protons Ar-H appeared in the range of 7.00 - 8.10 ppm, piperazine protons resonates at 1.50 - 3.80 ppm, methyl protons appeared in the range of 2.90 - 3.40 ppm, and methoxy protons $-\text{OCH}_3$ appeared in the range of 3.40 - 3.75 ppm. The ^1H NMR spectra of target compounds (A-L) are shown in supplementary information). Elemental analyses and ESI-MS spectra illustrated the compositions of the synthesized compounds. The mass spectra of A-L showed the peaks at m/z values of 490.24 , 490.24 , 490.24 , 517.23 , 472.24 , 552.16 , 476.23 , 476.23 , 538.15 , 458.23 , 503.22 and 476.23 corresponding

Benzyl halide	Product	Overall Yield (%)	Benzyl halide	Product	Overall Yield (%)
		57			52

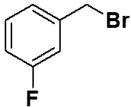
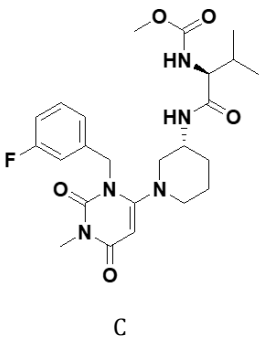
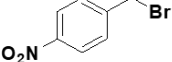
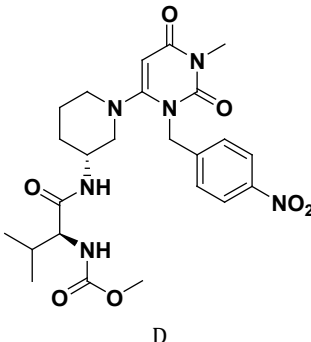
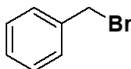
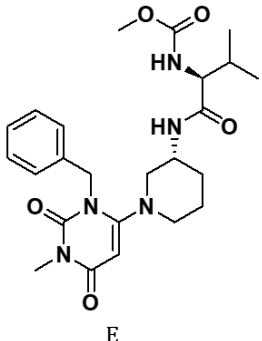
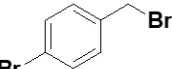
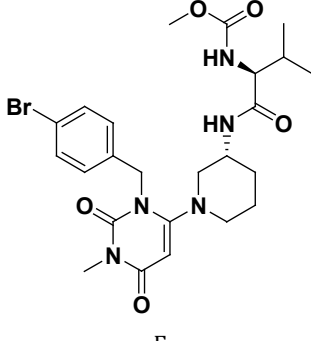
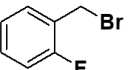
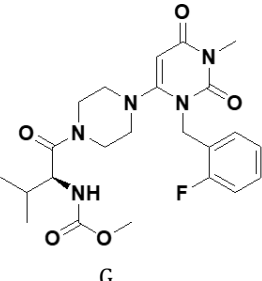
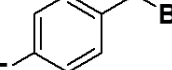
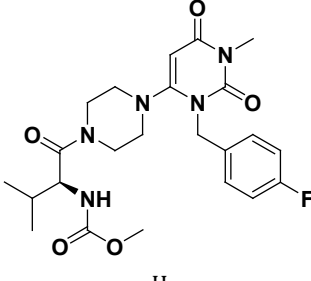
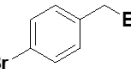
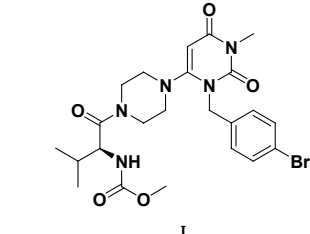
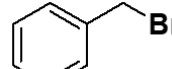
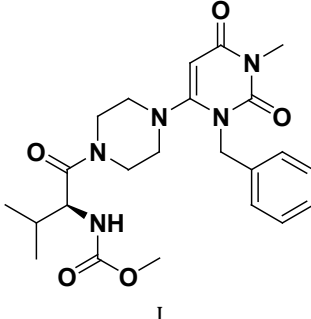
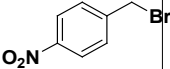
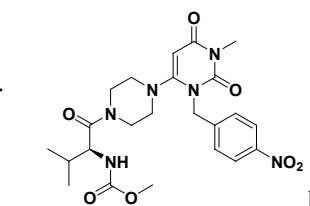
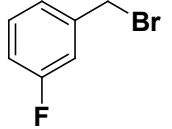
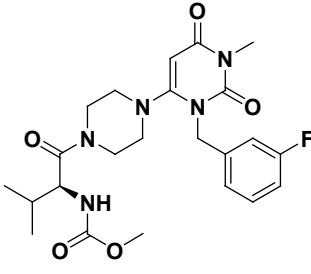
		51			59
		49			56
		56			57
		58			51
		60			60

Table 1: The chemical structures of initial and final coupled products.

to A, B, C, D, E, F, G, H, I, J, K and L. The HR-mass spectra of target compounds A-L are also given in supplementary information. The chemical structures of initial and final coupled products are given in table 1.

Methyl-(S)-1-((R)-1-(1-(3-(2-fluorobenzyl)-1-methyl-2,6-dioxo-1,2,3,6-tetrahydropyrimidin-4-yl)piperidin-3-ylamino)-3-methyl-1-oxobutan-2-ylcarbamate (A)

Yield: 57%, mp; 194-195 °C; White solid powder; Anal. Calcd: C (58.89), H (6.55), N (14.32%), Found: C (58.88), H (6.59), N (14.31%); ¹H-NMR (DMSO-d₆, 400 MHz): δ = 0.71-0.75 (dd, 6 H, -CH₃), 1.3-1.5 (m; 2 H, -CH₂), 1.72-1.77 (m, 3 H, -CH₂), 2.3-2.4 (t, 1 H, -CH₂), 2.6-2.7 (t, 1 H, -CH₂), 2.85-2.95 (d, 1H), 3.05 (s, 3 H, -N-CH₃), 3.1-3.2 (d, 1 H, -CH₂), 3.47 (s, 3 H, -O-CH₃), 3.70-3.74 (t, 2 H, -CH₂), 4.99-5.01 (q, 2 H, -CH₂), 5.26 (s, 1 H, -CH), 7.04-7.16 (M, 4 H, Ar-H, -NH), 7.25 (q, 1 H, Ar-H), 7.94-7.96 (d, 1 H, -NH); ES-MS (m/z) Calc. for C₂₄H₃₂FN₅O₅: 489.24, found [M+H]⁺: 490.24.

Methyl-(S)-1-((R)-1-(3-(4-fluorobenzyl)-1-methyl-2,6-dioxo-1,2,3,6-tetrahydropyrimidin-4-yl)piperidin-3-ylamino)-3-methyl-1-oxobutan-2-ylcarbamate (B)

Yield: 52%, mp; 230-231 °C; White solid powder; Anal. Calcd: C (58.87), H (6.57), N (14.29%), Found: C (58.88), H (6.59), N (14.31%); ¹H-NMR (DMSO-d₆, 400 MHz): δ = 0.72-0.76 (dd, 6 H, -CH₃), 1.29-1.50 (m; 2 H, -CH₂), 1.74-1.78 (m, 3 H, -CH₂), 2.3-2.4 (m, 1 H, -CH₂), 2.46-2.468 (s, 3 H, CH₂), 2.59-2.69 (m, 1 H, -CH₂), 2.8-2.9 (d, 1 H, -CH₂), 3.07-3.15 (s and broad, 4 H, -N-CH₃ and -CH), 3.48 (s, 3 H, -O-CH₃), 3.71-3.75 (t, 2 H, -CH₂), 4.93-4.97 (q, 2 H, -CH₂), 5.24 (s, 1 H, -CH), 7.07-7.11 (m, 3 H, Ar-H and -NH), 7.19-7.22 (m, 2 H, Ar-H), 7.97 (d, 1 H, -NH); ES-MS (m/z) Calc. for C₂₄H₃₂FN₅O₅: 489.54, found [M+H]⁺: 490.24.

Methyl-(S)-1-((R)-1-1-(3-(3-fluorobenzyl)-1-methyl-2,6-dioxo-1,2,3,6-tetrahydropyrimidin-4-yl)piperidin-3-ylamino)-3-methyl-1-oxobutan-2-ylcarbamate (C)

Yield: 51%, mp; 203-204 °C; White solid powder; Anal. Calcd: C (58.89), H (6.58), N (14.33%), Found: C (58.88), H (6.59), N (14.31%); ¹H-NMR (CDCl₃, 400 MHz): δ = 0.89- 0.90 (d, 6 H, -CH₃), 1.48-2.02 (m; 4 H, -CH₂), 2.47-2.86 (m, 3 H, -CH₂), 3.13-3.49 (m, 4 H, -N-CH₃ and -CH), 3.48 (s, 4 H, -O-CH₃ and -CH), 4.04 (broad, 1 H, -CH), 4.99-5.03 (d, 1 H, -CH), 5.11 (broad, 1 H, -CH), 5.23-5.33 (d, 2H, -Ar-CH₂), 5.84 (s, 1H, -CH-), 6.90-7.003 (m, 3 H, Ar-H), 7.26-7.33 (m, 1 H, Ar-H). ES-MS (m/z) Calc. for C₂₄H₃₂FN₅O₅: 489.54, found [M+H]⁺: 490.24.

Methyl-(S)-1-((R)-1-1-(3-(4-nitrobenzyl)-1-methyl-2,6-di-

oxo-1,2,3,6-tetrahydropyrimidin-4-yl)piperidin-3-ylamino)-3-methyl-1-oxobutan-2-ylcarbamate (D)

Yield: 59%, mp; 216-217 °C; White solid powder; Anal. Calcd: C (55.81), H (6.22), N (16.25%), Found: C (55.80), H (6.24), N (16.27%); ¹H-NMR (DMSO-d₆, 400 MHz): δ = 0.65-0.72 (dd, 6 H, -CH₃), 1.19-1.15 (t; 1 H, -CH₂), 1.29-1.42 (m, 2 H, -CH₂), 1.64-1.73 (m, 3 H, -CH), 2.464-2.468 (m, 1 H, -CH₂), 2.60-2.65 (m, 1 H, -CH₂), 2.83-2.86 (m, 1 H, -CH₂), 3.02-3.08 (m, 1 H, -CH₂), 3.30 (s, 3H, -CH₃), 3.47 (s, 3 H, -CH₃), 3.66-3.70 (t, 2 H, -CH₂), 5.03-5.16 (q, 2 H, -Ar-CH₂), 5.29 (s, 1 H, -CH), 7.06-7.09 (d, 1 H, -NH), 7.42-7.45 (d, 2H, Ar-H), 7.19-7.93 (d, 1 H, -NH), 8.12-8.15 (d, 2H, Ar-H) ppm; ES-MS (m/z) Calc. for C₂₄H₃₂N₆O₇: 516.55, found [M+H]⁺: 517.23.

Methyl-(S)-1-((R)-1-1-(3-benzyl-1-methyl-2,6-dioxo-1,2,3,6-tetrahydropyrimidin-4-yl)piperidin-3-ylamino)-3-methyl-1-oxobutan-2-ylcarbamate (E)

Yield: 49%, mp; 219-220 °C; White solid powder; Anal. Calcd: C (61.15), H (7.01), N (14.84%), Found: C, (61.13), H (7.05), N (14.85); ¹H-NMR (CDCl₃, 400 MHz): δ = 0.89-0.92 (t, 6 H, -CH₃), 1.50-1.64 (m; 2 H, -CH₂), 1.77-2.07 (m, 4 H, -CH₂), 2.5 (broad, 1 H, -CH), 2.76-2.88 (broad, 2 H, -CH), 3.30-3.34 (s, 4 H, -N-CH₃ and -CH), 3.69-3.76 (m, 4H, -OCH₃ and -CH), 4.06-4.08 (m, 1H, -CH-NH), 5.0-5.04 (ss, 1H, -CO-CH-NH), 5.28-5.34 (m, 3H, -Ph-CH₂ and =CH-), 7.20-7.22 (d, 2H, Ar-H), 7.27-7.30 (t, 1H, Ar-H), 7.34-7.38 (t, 2H, -Ar-H) ppm; ES-MS (m/z) Calc. for C₂₄H₃₃N₅O₅: 471.55, found [M+H]⁺: 472.24.

Methyl-(S)-1-((R)-1-(1-(3-(4-bromobenzyl)-1-methyl-2,6-dioxo-1,2,3,6-tetrahydropyrimidin-4-yl)piperidin-3-ylamino)-3-methyl-1-oxobutan-2-ylcarbamate (F)

Yield: 56%, mp; 210-212 °C; White solid powder; Anal. Calcd: C (52.34), H (5.84), N (12.71%), Found: C (52.37), H (5.86), N (12.72%); ¹H-NMR (DMSO-d₆, 400 MHz): δ = 0.70-0.76 (dd, 6 H, -CH₃), 1.31-1.44 (m; 2 H, -CH₂), 1.75-1.80 (m, 3H, -CH₂), 2.65 (m, 2H, -CH₂), 2.83 (t, 1 H, -CH₂), 3.30 (s, 3 H, -CH₃), 3.47 (s, 3H, -CH₃), 3.70-3.73 (t, 2H, -CH₂), 4.86-5.001 (q, 1H, -Ar-CH₂), 5.24 (s, 1H, -CH), 7.11-7.12 (d, 2H, Ar-H), 7.45-7.47 (d, 2H, A-H), 7.95-7.96 (d, 1H, -NH) ppm; ES-MS (m/z) Calc. for C₂₄H₃₂BrN₅O₅: 550. 45, found [M+H]⁺: 552.16.

(S)-Methyl-1-(4-(3-(2-fluorobenzyl)-1-methyl-2,6-dioxo-1,2,3,6-tetrahydropyrimidin-4-yl)piperazin-1-yl)-3-methyl-1-oxobutan-2-ylcarbamate (G)

Yield: 56%, mp; 161-164 °C; White solid powder; Anal. Calcd: C (58.07), H (6.33), N (14.71%), Found: C, (58.09), H (6.36), N (14.73%); ¹H-NMR (DMSO-d₆, 400 MHz): δ = 0.80-0.95 (d, 3 H, -CH₃), 1.12-1.34 (m, 2 H, -CH₂), 1.92-1.94 (m, 1 H, -CH₂), 2.81-2.88

(m, 4 H, -CH₂), 3.12 (s, 3 H, -CH₃), 3.36 (m, 4 H, -CH₂), 3.53-3.64 (m, 4H and 2H, -OCH₃, -CH₂ & -CH), 4.22-4.26 (m, 1H, -CH), 5.10 (s, 2 H, -CH₂), 5.39 (s, 1 H, -CH), 7.17-7.22 (m, 3 H, Ar-H), 7.31-7.33 (m, 2H, Ar-H); ES-MS (m/z) Calc. for C₂₃H₃₀FN₅O₅: 475.22, found [M+H]⁺: 476.23.

(S)-Methyl-1-(4-(3-(4-fluorobenzyl)-1-methyl-2,6-dioxo-1,2,3,6-tetrahydropyrimidin-4-yl)piperazin-1-yl)-3-methyl-1-oxobutan-2-ylcarbamate (H)

Yield: 57%, mp; 217-219 °C; White solid powder; Anal. Calcd: C (58.09), H (6.32), N (14.72%), Found: C (58.09), H (6.36), N (14.73%); ¹H-NMR (DMSO-d₆, 400 MHz): δ = 0.85 (d, 6 H, -CH₃), 1.92 (m, 1 H, -CH₂), 2.65-2.69 (m, 4 H, -CH₂), 2.84 (broad, 4 H, CH₂), 3.13 (s, 3 H, -N-CH₃), 3.35 (broad, 6H, -O-CH₃ & -CH₂), 3.53 (broad, 4 H, -CH₂), 3.66 (broad, 2 H, -CH₂), 4.22-4.26 (t, 1 H, -CH), 5.04 (s, 2 H, Ar-CH₂), 5.37 (s, 1 H, -CH), 7.14-7.18 (t, 2 H, Ar-H), 7.30-7.34 (m, 3 H, Ar-H, and -NH); ES-MS (m/z) Calc. for C₂₃H₃₀FN₅O₅: 475.51, found [M+H]⁺: 476.23.

(S)-Methyl-1-(4-(3-(4-bromobenzyl)-1-methyl-2,6-dioxo-1,2,3,6-tetrahydropyrimidin-4-yl)piperazin-1-yl)-3-methyl-1-oxobutan-2-ylcarbamate (I)

Yield: 58%, mp; 234-233 °C; White solid powder; Anal. Calcd: C (51.51), H (5.62), N (13.04%), Found: C (51.50), H (5.64), N (13.06%); ¹H-NMR (DMSO-d₆, 400 MHz): δ = 0.83-0.86 (t, 6 H, -CH₃), 1.91-1.96 (m; 1 H, -CH₂), 2.69 (s, 3H, -CH₃), 2.85-2.90 (broad, 4H, -CH), 3.13 (s, 3 H, -CH₃), 3.35(s, 4 H), 3.53 (s, 3H), 3.66 (broad, 2H), 4.23-4.27(t, 1H), 5.03 (s, 2H, -Ar-CH₂), 5.37(s, 1H, -CH), 7.20-7.22 (d, 2H, Ar-H), 7.28-7.30 (d, 1H, -NH) 7.51-7.53 (d, 2H, Ar-H) ppm; ES-MS (m/z) Calc. for C₂₃H₃₀BrN₅O₅: 536.42, found [M+H]⁺: 538.15.

(S)-Methyl 1-(4-(3-benzyl-1-methyl-2,6-dioxo-1,2,3,6-tetrahydropyrimidin-4-yl)piperazin-1-yl)-3-methyl-1-oxobutan-2-ylcarbamate (J)

Yield: 51%, mp; 173-174 °C; White solid powder; Anal. Calcd: C (60.39), H (6.82), N (15.32%), Found: C (60.38), H (6.83), N (15.31%); ¹H-NMR (DMSO-d₆, 400 MHz): δ = 0.78-0.81 (t, 6 H, -CH₃), 1.84-1.92 (m; 1 H, -CH₂), 2.65 (s, 2H), 2.79-2.82 (broad, 4 H, -CH), 3.10 (s, 3 H, -CH₃), 3.31 (s, 3H, -OCH₃), 3.60-3.66 (broad, 2H), 4.17-4.21(t, 1H), 5.02 (s, 2H, -Ar-CH₂), 5.33 (s, 1H, -CH) 7.18-7.23 (m, 3H, Ph), 7.27-7.31 (t, 2H, Ph)ppm; ES-MS (m/z) Calc. for C₂₃H₃₁N₅O₅: 457.52, found [M+H]⁺: 458.23.

(S)-Methyl-1-(4-(3-(4-nitrobenzyl)-1-methyl-2,6-dioxo-1,2,3,6-tetrahydropyrimidin-4-yl)piperazin-1-yl)-3-methyl-1-oxobutan-2-ylcarbamate (K)

Yield: 60%, mp; 205-206 °C; White solid powder; Anal. Calcd: C (54.95), H (6.00), N (16.70%), Found: C (54.97), H (6.02), N (16.72%); ¹H-NMR (CDCl₃, 400 MHz): δ = 0.93-0.97 (dd, 6 H, -CH₃), 1.27-1.30 (d, 1H, -CH), 1.91-1.96 (q, 1 H, -CH), 2.81 (s, 5 H, -N-CH₃, CH₂), 2.90 (broad, 3H,) 3.33(s, 3 H, -O-CH₃), 4.41-4.45 (q, 1H, -CH), 5.21 (s, 2H, Ar-CH₂), 5.42-5.47 (t, 2 H), 7.38-7.40 (d, 2 H, -Ar H), (d, 2 H, -Ar-H), ppm; ES-MS (m/z) Calc. for C₂₃H₃₀N₆O₇: 502.52, found [M+H]⁺: 503.22.

(S)-Methyl-1-(4-(3-(3-fluorobenzyl)-1-methyl-2,6-dioxo-1,2,3,6-tetrahydropyrimidin-4-yl)piperazin-1-yl)-3-methyl-1-oxobutan-2-ylcarbamate (L)

Yield: 60%, mp; 220-222 °C; White solid powder; Anal. Calcd: C (58.09), H (6.34), N (14.73%), Found: C (58.09), H (6.36), N (14.73%); ¹H-NMR (DMSO-d₆, 400 MHz): δ = 0.71-0.76 (dd, 6 H, -CH₃), 1.3-1.5 (m; 2 H, -CH₂), 1.74-1.79 (m, 3 H, -CH₂), 2.30-2.46 (m, 4 H, -CH), 2.59 (m, 1 H, -CH₂), 2.80-2.9(m, 1 H, -CH₂), 3.08 (s, 3 H, -N-CH₃), 3.48 (s, 3 H, -CH₃), 3.74-3.75 (t, 2 H, -CH₂), 4.92-5.04 (d, 2 H, -Ar-CH₂), 5.25 (s, 1 H, -CH), 6.99-7.05 (m, 3 H, -Ar-H), 7.09-7.11 (d, 1 H, -NH), 7.29-7.34 (q, 1 H, -Ar-H), 7.95-7.96 (d, 1 H, -NH) ppm. ES-MS (m/z) Calc. for C₂₃H₃₀FN₅O₅: 475.521, found [M+H]⁺: 476.23.

DNA binding study

The absorption spectra of compounds (F, G, and H; 2.0 × 10⁻³ M) in both absence and presence (0.2 – 1.4 × 10⁻³ M) of Ct-DNA is given in figure 5. The absorption spectra of compounds exhibited peaks in the range of 200-300 nm. The compounds A-L showed two absorption bands, the first band appeared at 235-260 nm and the second band appeared at 269 – 296 nm, respectively. The band shifting was observed in the region of 200-300 nm with the addition of DNA. Almost in all cases of A-L, both types of shifting in bands (hypochromism and bathochromism) i.e. very small and large was observed. Moreover, the appearances of isosbestic points in titration experiments also showed the interaction of compounds with Ct-DNA. UV-vis data for compounds A-L (Table 2). The values of DNA binding constants of these compounds varied from 6.0 × 10⁵ to 9.0 × 10⁷ M⁻¹. The order of DNA binding constants for compounds A-L was G>H>F>B>C>A>L>I>D>J>E. It was very interesting to note

(A)

(B)

(C)

Figure 5: Absorption spectra of compound (a) F (b) G and (c) H [2.0×10^{-3} M], in the absence and presence of DNA. The concentration of DNA (a-f) were 0, 0.2, 0.4, 0.6, 0.8, 1.2 and 1.4×10^{-3} M.

that the compounds containing halogen groups (fluoro, bromo) (A, B, C, F, G, H, I and L) had the highest affinity for DNA (higher K_b values). On the other hand, compounds containing the nitro group had a better affinity towards DNA, than other compounds. These results are in the agreement with the earlier reported work [44].

Compounds	$\lambda_{\max}^{\text{free}}$ (nm)	$\lambda_{\max}^{\text{bound}}$ (nm)	$\Delta\lambda_{\max}$ (nm)	% Hypochromism ^a	K_b^b (M^{-1})
A	260, 290	262, 292	2	1.0	6.1×10^7
B	236, 267	238, 269	2	2.3	7.1×10^7
C	235, 294	236, 295	1	5.2	6.7×10^7
D	245, 295	246, 296	1	1.0	4.6×10^6
E	236, 272	238, 274	2	2.3	6.0×10^5
F	235, 267	235, 282	20	6.8	7.8×10^7
G	236, 269	236, 279	10	7.1	9.0×10^7
H	234, 259	234, 279	20	48	8.0×10^7
I	242, 296	244, 298	2	3.1	4.9×10^7
J	257, 291	259, 293	2	2.9	8.8×10^5
L	245, 296	246, 297	0	0.5	5.8×10^7

Table 2: UV absorption, wavelength shifts, % hypochromism and binding constants of A-L.

^a % Hypochromicity (H%) = $[A_f - A_b]/A_f \times 100$, where A_f and A_b represent the absorbance of free and bound compounds. ^b Binding constants.

Docking study

The order of binding affinities of the selected compounds was found $G > H > F$. The 3D and 2D-docked models of F, G and H are shown in figure 6-11. It is clear from the docked models that all the compounds preferred DNA minor grooves. The various docking parameters like binding affinity, number of H-bonds and residues involved in H-bonding, and in hydrophobic interactions are given in table 3. During the docking studies, it was observed that the carbonyl oxygen of the amide group and oxygen of the ethoxy group of DNA were the common moieties involved in H-bonding. The number of hydrogen bonds formed was 3 to 4. The DNA residues; guanine and cytosine were involved in hydrogen bonding. Furthermore, DNA residues like dt8, dc9, dg10, dc13, dg14, dc15,

Figure 6: 3D-Docking images of compound F with CT-DNA. (a) shows the interaction via minor groove, (b) Closest view within the groove and (c) indicate polar interactions.

Figure 7: 2D-Docking images of compound F with CT-DNA. (a and b) shows the moieties of DNA involved in hydrophobic interactions.

Figure 8: 3D-Docking images of compound G with CT-DNA. (a) shows the interaction via minor groove, (b) Closest view within the groove and (c) indicate polar interactions.

Figure 9: 2D-Docking images of compound G with CT-DNA. (a and b) shows the moieties of DNA involved in hydrophobic interactions.

Figure 10: 3D-Docking images of compound H with CT-DNA. (a) shows the interaction via minor groove, (b) Closest view within the groove and (c) indicate polar interactions.

Figure 11: 2D-Docking images of compound H with CT-DNA. (a and b) shows the moieties of DNA involved in hydrophobic interactions.

Target (pdb code)	Drugs	Binding affinity (kJ/mol)	No of H-bonds	H-bonding rsidues (Bond length in Å°)	Target::drug hydrophobic residues
DNA (1bna)	F	-3.8	4	A/DG:10/H01::O of carbonyl of uracil ring (3.30). A/DG:14/H06::O of carbonyl of uracil ring (3.32). B/DG:14/OP2::NH of 3-aminopiperidine moiety (3.25). B/DG:14/PO2::NH of other amine group (3.39).	dt8::C12&C13 dc9::C8,C13&C18 dg10::C13&C18 dc13::Br dg14::C3,C4,C7&O4 dc15::C8,C9&C14 dg16::C8.
	G	-4.7	3	B/DG:14/H02::O of carbonyl of ester group (3.46). B/DC:15/H01:: O of carbonyl linked to piperazine ring (3.38). B/DG:14/H02:: O of carbonyl linked to piperazine ring (3.39).	dt8::C6,C7,C16&O2 dc9::O1 dg10::O1 dc13::C4&C5 dg14::C4,C11&C13 dc15::C11&C17
	H	-4.0	4	B/DG:14/H01::O of carbonyl linked to piperazine ring ((3.48). B/DG:14/H01:: O of carbonyl linked to piperazinerings(3.52). B/DG:14/H02::O of carbonyl of ester group (3.30). B/DG:16/H01::O of carbonyl of ester group (3.31).	dt8::C4 dc9::C1,C4,C6,C7&C17 dg10::C3&C16 dg14::C10&C12 dc15::C1,C4,C16&O4 dg16::C4

RTs (2rf2)	A	-3.8	2	.159/A/GLN`197/2HE2::O of -CONH2 group (2.7) .648/A/GLU`194/OE1::O of -CONH2 (3.4).	Asp192::C1,C8,C9,C17&C18 Glu194::C13,C22,C24&O1 Gln197::O4
	B	-2.4	1	.274/A/LYS`104/HZ2::O of -CO- group (2.7)	Asp192::C2,C4,C8&C18 Glu194::C11,C12&C16 Lys104::C2,C17 & O2 Leu193::C6
	C	-2.5	1	.274/A/LYS`104/HZ2::O of -CO- group (2.7)	Asp192::C1,C3,C6&C17 Glu194::C11,C15&C23 Lys104::C1,C17&O2
	D	-2.4	1	.274/A/LYS`104/HZ2 ::O of -CO- group (2.6)	Asp192::C2,C4,C8&C18 Glu194::C11,C12&C16 Lys104::C18,C23,O2&N5
	E	-2.5	1	.274/A/LYS`104/HZ2::O of -CO- group (2.7)	Asp192::C6,C7,C8,C9,C13&C18 Glu194::C12,C13,C16&C21 Lys104::C8,C23,N4&O2
	F	-2.5	1	.648/A/ASP`320/OD2::O of -CO- group (3.6)	Asp192::C2,C4&C8 Glu194::C8,C12,C13&C16 Lys104::C18,C23&O2
	G	-3.1	1	.648/A/GLU`194/OE2::O of -CO- group (3.6)	Asp192::C5,C8,C13&C18 Ser322::C2&C3 Lys102::C15,C21,C22&O5 Asp320::C1&C6
	H	-2.6	2	.274/A/LYS`104/HZ1::O of -CONH- group (2.7) .648/A/GLU`194/OE2::O of -CONH- group (3.3)	Asp192::C1,C16&N3 Glu194::C1,C6,C20,C23&O1 Lys104::C13 & O4
	I	-2.5	1	.274/A/LYS`104/HZ1:: O of -COO- group (2.4)	Asp192::C16,C17,C21,O2 N2&N3 Glu194::C2,C5,C14,C18,C23&O1 Lys104::C12 & C14
	J	-2.8	3	.271/A/ASP`192/O:: O of -CO- group (3.4) .648/A/ASP`320/OD2:: O of -COO- group (3.4) .648/A/ASP`320/OD2:: O of -CONH- group (3.5)	Asp192::C11,C15,C16,C17, C22,O2,N2&N3 Ser322::C8&C9 Lys104::O2
	K	-2.9	3	.274/A/LYS`104/HZ2:: O of -CONH- group (2.0) .648/A/GLU`194/OE2:: O of -COO- group (3.2) .271/A/ASP`192/O:: O of -NO2 group (3.4)	Asp192::C1,C2,C3,C6,C7,C12&O7 Glu194::C23 Lys104::O4
	L	-2.9	Nil	Nil	Asp192::C1,C3,C4&C7 Glu194::C2,C3,C9,C11,C14,C15, C22&N2 Leu104::C1

Table 3: The docking results of newly synthesized drugs with DNA and RTs.

RTs: Reverse transcriptase; dc: cytosine; dg: guanine; dt: thiamine.

and dg16 were involved in hydrophobic interactions. During the process of DNA interaction, it was observed that all the target compounds oriented themselves in such a fashion that their benzene rings were inside minor grooves. Overall, the experimental results of DNA binding and theoretical docking results were found in good covenant with each other.

In the case of RTs of HIV, it was perceived that all newly synthesized drugs attack on that side of the receptor where the residue, Lys is present specifically. The number of hydrogen bonds formed by newly synthesized drugs with RTs enzyme, was 2 in the case of A and H; 1 in the case of B-G and I; 3 in the case of J and K, while L did

Figure 12: The attachments of newly synthesized drugs with RTs.

Figure 13: The hydrophobic interactions of newly synthesized drugs with RTs.

not form any hydrogen bond (Figure 12). Another observable point was the binding affinities of compound A-L with RTs of HIV. The average of the binding affinities of newly synthesized drugs (A-L) was -2.4 to -3.8 k cal/mol (Table 3). Besides, the common residues of newly synthesized drugs involved in the hydrophobic interactions with RTs enzyme were Lys, Glu, Leu, Asp, Ser (Figure 13).

Discussion

The values of DNA binding constants of newly synthesized drugs indicate good interaction with DNA. As per the results of the DNA binding study and docking study of the selected three compounds, the compound G would exhibit better anticancer activity because

the binding affinity of G towards DNA was greater than that of other newly synthesized drugs. The small shifting occurs due to intra ligand $\pi \rightarrow \pi^*$, while the large shifting due to $n \rightarrow \pi^*$ transitions of the compounds [45]. It was also observed that the absorption peaks underwent bathochromism and hypo-chromicities (Figure 5) with the addition of different concentrations of DNA [$0.2 - 1.2 \times 10^{-3}$ M]. It indicates the formation of DNA-compound adducts *via* intercalative mode (non-covalent) [46]. It can be concluded from the DNA binding results that the compounds A-L intercalated through the minor groove with Ct-DNA [47]. Literature data indicate that the compound, forming a complex with DNA minor groove, is stabilized mainly by hydrogen bonds and hydrophobic interactions

[48]. This fact is well established by DNA titration experiments and docking studies (Figure 6-11). Moreover, the observation of isosbestic points in mixed solutions also indicates the interaction of the newly synthesized drugs with DNA molecules. Covalent (i.e. a labile ligand is replaced with a nitrogen atom of DNA base, such as N7 of guanine) and non-covalent (i.e. intercalation, electrostatic interaction, and groove binding) interactions are the two possible ways through which a compound can bind with DNA. Normally, in absorption spectra, the changes like hypochromism and bathochromism resulted when compounds bind to DNA *via* intercalation, and the extent of hypochromism depends on the strength of intercalation [36,44,49-52]. Basically, the interactive mode involved a strong stacking interaction between the aromatic chromophore of the drug and the base pairs of DNA [52,53]. While, in electrostatic interaction when the drug interacts with DNA, lower hypochromicity with no bathochromic shift [54] or hyperchromic shift is observed [55]. The hyperchromic effect was not observed in the absorbance of DNA, which occurs due to the covalent adducts formed between drugs and DNA. If hyperchromism was observed, it would be the indication of breakage of the secondary structure of DNA [56].

On the other hand, as per the docking results, all newly synthesized drugs showed their attachment with different residues. The most important residue that was common in the case of newly synthesized drugs, and plays a key role in the synthesis of viral protein, was Lys (Lysine) specifically. A huge association between lysine and HIV-1 RNA replication has been found. The synthesis of viral protein needs lysine too much, and it may increase the risk of high viral load, subsequent acceleration of immunosuppression and HIV progression [57]. The role of lysine in the synthesis of viral protein is not common in all types of viruses such as herpesvirus [58], but its crucial role was found especially in HIV-1 [57] and Reovirus [59]. Hence, as per docking results and literature data [57,59], newly derived compounds if used against HIV, will interact with the most important residue (Lys) of RTs to interfere in the synthesis of viral protein. Hence, due to the disruption in the crucial residue (Lys), HIV-1 would not synthesize its protein, and unable to replicate itself. Moreover, the involvement of the same residue i.e. Lys of RTs enzyme with anti-HIV drugs other than the newly synthesized drugs, have also been confirmed experimentally [43,60]. Hence, the docking study predicts the attachment of newly synthesized drugs on that side of RTs enzyme where the residue playing a key role

in the protein synthesis and replication, is present. Besides, another notable point was the binding affinities of newly synthesized drugs. As per the docking results, the binding affinity of A towards RTs was greater than that of other newly synthesized drugs, it predicts that drug A would bind with RTs more tightly as compared to other newly synthesized drugs. Hence, drug A would be a more effective drug than other newly synthesized drugs.

Conclusions

We developed a new, efficient, low-cost, eco-friendly, highly scalable one-pot method for the synthesis of new uracil derivatives. Based on literature data, DNA binding study and docking studies, it can be concluded that these compounds may play a key role in the treatment of not only cancer and but also AIDS. Besides, a trial of these drugs may also be taken against SARS-Cov-2, because uracil derivatives have also been used against the same as per the introductory part of the article.

Author Contributions

Vadivelan Rengasamy conceived and designed the study, and wrote the manuscript under the supervision of Arvind Jain. Mohd. Suhail did DNA binding study and computational study. Besides, he also reviewed and edited the manuscript. All data were generated in-house, and no paper mill was used. All authors agree to be accountable for all aspects of the work, ensuring integrity and accuracy.

Declaration of Competing Interest

We wish to confirm that there are no known conflicts of interest

Bibliography

1. Shah A., *et al.* "Photochemistry and Electrochemistry of Anti-cancer Uracils". *Journal of Photochemistry and Photobiology B: Biology* 117 (2012): 269-277.
2. Wu C., *et al.* "Antitumor Activity of Combination Treatment of Lentinus Edodes Mycelium Extracts with 5-Fluorouracil against Human Colon Cancer Cells Xenografted in Nude Mice". *Journal of Cancer Molecules* 3.1 (2007): 15-22.
3. de Berker D., *et al.* "Guidelines for the Management of Actinic Keratoses". *British Journal of Dermatology* 156.2 (2007): 222-230.

4. Ardalan B., *et al.* "Biomodulation of Fluorouracil in Colorectal Cancer". *Cancer Investigation* 16.4 (1998): 237-251.
5. Freelove R and Walling A D. "Pancreatic Cancer: Diagnosis and Management". *American Family Physician* 73.3 (2006): 485-492.
6. Saonere J A. "Awareness Screening Programme Reduces the Risk of Cervical Cancer in Women". *African Journal of Pharmacy and Pharmacology* 4.6 (2010): 314-323.
7. Choi. "5-Fluorouracil Combined with Apigenin Enhances Anticancer Activity through Induction of Apoptosis in Human Breast Cancer MDA-MB-453 Cells". *Oncology Reports* 22.06 (2009).
8. Longley D B., *et al.* "5-Fluorouracil: Mechanisms of Action and Clinical Strategies". *Nature Reviews Cancer* 3.5 (2003): 330-338.
9. Maruyama T., *et al.* "Antiviral Activity of 3-(3,5-Dimethylbenzyl)Uracil Derivatives Against Hiv-1 and HCMV". *Nucleosides, Nucleotides and Nucleic Acids* 26.10-12 (2007): 1553-1558.
10. Bertoletti N., *et al.* "Structural Insights into the Recognition of Nucleoside Reverse Transcriptase Inhibitors by "HIV-1 Reverse Transcriptase: First Crystal Structures with Reverse Transcriptase and the Active Triphosphate Forms of Lamivudine and Emtricitabine". *Protein Science* 28.9 (2019): 1664-1675.
11. Hung M., *et al.* "Elucidating Molecular Interactions of L-Nucleotides with HIV-1 Reverse Transcriptase and Mechanism of M184V-Caused Drug Resistance". *Communications Biology* 2.1 (2019): 469.
12. Pałasz A and Cieź D. "In Search of Uracil Derivatives as Bioactive Agents. Uracils and Fused Uracils: Synthesis, Biological Activity and Applications". *European Journal of Medicinal Chemistry* 97 (2015): 582-611.
13. Abdel-Mottaleb Y and Abdel-Mottaleb M S A. "Molecular Modeling Studies of Some Uracil and New Deoxyuridine Derivatives". *Journal of Chemistry* 2016 (2016): 1-12.
14. Awad S M., *et al.* "Synthesis and Evaluation of Some Uracil Nucleosides as Promising Anti-Herpes Simplex Virus 1 Agents". *Molecules* 26.10 (2021): 2988.
15. Kim Y., *et al.* "Tipiracil Binds to Uridine Site and Inhibits Nsp15 Endoribonuclease NendoU from SARS-CoV-2". *Communications Biology* 4.1 (2021): 193.
16. Pillon M C., *et al.* "Cryo-EM Structures of the SARS-CoV-2 Endoribonuclease Nsp15 Reveal Insight into Nuclease Specificity and Dynamics". *Nature Communications* 12.1 (2021): 636.
17. Kim Y., *et al.* "Crystal Structure of Nsp15 Endoribonuclease <scp>NendoU</Scp> from <scp>SARS-CoV</Scp> -2". *Protein Science* 29.7 (2020): 1596-1605.
18. Yin W., *et al.* "Structural Basis for Inhibition of the RNA-Dependent RNA Polymerase from SARS-CoV-2 by Remdesivir". *Science* 368.6498 (2020): 1499-1504.
19. Imran A., *et al.* "Anti-Cancer and Anti-Oxidant Potencies of Cuscuta Reflexa Roxb . Plant Extracts". *American Journal of Advanced Drug Deliverycan Journal of Advanced Drug Delivery* 14.2 (2019): 92-113.
20. Ali I., *et al.* "Role of Unani Medicines in Cancer Control and Management". *Current Drug Therapy* 14. 2 (2019): 92-113.
21. Suhail M and Ali I. "An Advanced Computational Evaluation for the Most Biologically Active Enantiomers of Chiral Anti-Cancer Agents". *Anti-Cancer Agents in Medicinal Chemistry* 21 (2020).
22. Ali I., *et al.* "Advances in Nanocarriers for Anticancer Drugs Delivery". *Current Medicinal Chemistry* 23.20 (2016) 2159-2187.
23. Murinov Y I., *et al.* "Pro- and Antioxidant Properties of Uracil Derivatives". *Russian Chemical Bulletin* 68.5 (2019): 946-954.
24. Feng J., *et al.* "Discovery of Alogliptin: A Potent, Selective, Bioavailable, and Efficacious Inhibitor of Dipeptidyl Peptidase IV †". *Journal of Medicinal Chemistry* 50.10 (2007): 2297-2300.
25. Ma H., *et al.* "Characterization of the Metabolic Activation of Hepatitis C Virus Nucleoside Inhibitor β -d-2'-Deoxy-2'-Fluoro-2'-C-Methylcytidine (PSI-6130) and Identification of a Novel Active 5'-Triphosphate Species". *Journal of Biological Chemistry* 282.41 (2007): 29812-29820.
26. Bergstrom D E. "Organometallic Intermediates in the Synthesis of Nucleoside Analogs". *Nucleosides and Nucleotides* 1.1 (1982): 1-34.
27. Hayashi Y. "Pot Economy and One-Pot Synthesis". *Chemical Science* 7.2 (2016) 866-880.
28. Christensen S., *et al.* "5-Fluorouracil Treatment Induces Characteristic T&gT;G Mutations in Human Cancer". *Nature Communications* 10.1 (2019): 4571.

29. De Almeida C V., *et al.* "Treatment of Colon Cancer Cells with 5-Fluorouracil Can Improve the Effectiveness of RNA-Transfected Antitumor Dendritic Cell Vaccine". *Oncology Reports* 38.1 (2017): 561-568.
30. Kennard O. "DNA-Drug Interactions". *Pure and Applied Chemistry* 65.6 (1993): 1213-1222.
31. Barton J K., *et al.* "Tris(Phenanthroline)Ruthenium(II): Stereoselectivity in Binding to DNA". *Journal of the American Chemical Society* 106.7 (1984): 2172-2176.
32. Sun H., *et al.* "A Stabilizing and Denaturing Dual-Effect for Natural Polyamines Interacting with G-Quadruplexes Depending on Concentration". *Biochimie* 93.8 (2011): 1351-1356.
33. Jaumot J and Gargallo R. "Experimental Methods for Studying the Interactions between G-Quadruplex Structures and Ligands". *Current Pharmaceutical Design* 18.14 (2012): 1900-1916.
34. Wei C., *et al.* "Spectroscopic Study on the Binding of Porphyrins to (G4T4G4)4 Parallel G-Quadruplex". *Biophysical Chemistry* 148.1-3 (2010): 51-55.
35. Bhadra K and Kumar GS. "Interaction of Berberine, Palmatine, Coralyne, and Sanguinarine to Quadruplex DNA: A Comparative Spectroscopic and Calorimetric Study". *Biochimica et Biophysica Acta (BBA) - General Subjects* 1810.4 (2011): 485-496.
36. Liu X W., *et al.* "Experimental and DFT Studies on the DNA-Binding Trend and Spectral Properties of Complexes [Ru(Bpy)2L]2+ (L=dmdpq, Dpq, and Dcdpq)". *Inorganica Chimica Acta* 358. 12 (2005): 3311-3319.
37. Benesi H A and Hildebrand J H. "A Spectrophotometric Investigation of the Interaction of Iodine with Aromatic Hydrocarbons". *Journal of the American Chemical Society* 71.8 (1949): 2703-2707.
38. Wolfe A., *et al.* "Polycyclic Aromatic Hydrocarbons Physically Intercalate into Duplex Regions of Denatured DNA". *Biochemistry* 26.20 (1987): 6392-6396.
39. Morris G M., *et al.* "AutoDock4 and AutoDockTools4: Automated Docking with Selective Receptor Flexibility". *Journal of Computational Chemistry* 30.16 (2009): 2785-2791.
40. Trott O and Olson A J. "AutoDock Vina: Improving the Speed and Accuracy of Docking with a New Scoring Function, Efficient Optimization, and Multithreading". *Journal of Computational Chemistry* 31.2 (2010): 455-461.
41. Laskowski R A and Swindells M B. "LigPlot+: Multiple Ligand-Protein Interaction Diagrams for Drug Discovery". *Journal of Chemical Information and Modeling*, 51.10 (2011): 2778-2786.
42. Drew H R., *et al.* "Structure of a B-DNA Dodecamer: Conformation and Dynamics". *Proceedings of the National Academy of Sciences of the United States of America* 78.4 (1981): 2179-83.
43. Zhao Z., *et al.* "Novel Indole-3-Sulfonamides as Potent HIV Non-Nucleoside Reverse Transcriptase Inhibitors (NNRTIs)". *Bioorganic and Medicinal Chemistry Letters* 18.2 (2008): 554-559.
44. Pyle A M., *et al.* "Mixed-Ligand Complexes of Ruthenium(II): Factors Governing Binding to DNA". *Journal of the American Chemical Society* 111.8 (1989): 3051-3058.
45. Chen LM., *et al.* "Synthesis, Characterization, DNA-Binding and Spectral Properties of Complexes [Ru(L)4(Dppz)]2+ (L=Im and MeIm)". *Journal of Inorganic Biochemistry* 102.2 (2008): 330-341.
46. Zhao P., *et al.* "Experimental and DFT Studies on DNA Binding and Photocleavage of Two Cationic Porphyrins". *Spectrochimica Acta Part A: Molecular and Biomolecular Spectroscopy* 71.4 (2008): 1216-1223.
47. Arjmand F., *et al.* "Molecular Drug Design, Synthesis and Crystal Structure Determination of CuII-SnIV Heterobimetallic Core: DNA Binding and Cleavage Studies". *European Journal of Medicinal Chemistry* 49 (2012): 141-150.
48. Haq I. "Thermodynamics of Drug-DNA Interactions". *Archives of Biochemistry and Biophysics* 403.1 (2002): 1-15.
49. Liu X-W., *et al.* "Synthesis, Characterization, DNA-Binding and Photocleavage of Complexes [Ru(Phen)2(6-OH-Dppz)]2+ and [Ru(Phen)2(6-NO2-Dppz)]2+". *Journal of Inorganic Biochemistry* 99.12 (2005): 2372-2380.
50. Sirajuddin M., *et al.* "Drug-DNA Interactions and Their Study by UV-Visible, Fluorescence Spectroscopies and Cyclic Voltammetry". *Journal of Photochemistry and Photobiology B: Biology* 124 (2013): 1-19.
51. Sirajuddin M., *et al.* "Synthesis, Characterization, Biological Screenings and Interaction with Calf Thymus DNA of a Novel Azomethine 3-[(3,5-Dimethylphenylimino)Methyl] Benzene-1,2-Diol". *Spectrochimica Acta Part A: Molecular and Biomolecular Spectroscopy* 94 (2012): 134-142.

52. Shahabadi N., *et al.* "DNA Interaction Studies of a Platinum(II) Complex, PtCl₂(NN) (NN=4,7-Dimethyl-1,10-Phenanthroline), Using Different Instrumental Methods". *Spectrochimica Acta Part A: Molecular and Biomolecular Spectroscopy* 72.4 (2009): 757-761.
53. Indumathy R., *et al.* "Cobalt Complexes of Terpyridine Ligands: Crystal Structure and Nuclease Activity". *Polyhedron* 27.17 (2008): 3443-3450.
54. Arjmand F and Jamsheera, A. "DNA Binding Studies of New Valine Derived Chiral Complexes of Tin(IV) and Zirconium(IV)". *Spectrochimica Acta Part A: Molecular and Biomolecular Spectroscopy* 78.1 (2011): 45-51.
55. Allardyce C S., *et al.* "[Ru(H₆-p-Cymene)Cl₂(Pta)] (Pta = 1,3,5-Triaza-7-Phosphatrimethylcyclo[3.3.1.1]Decane): A Water Soluble Compound That Exhibits PH Dependent DNA Binding Providing Selectivity for Diseased Cells". *Chemical Communications* 15 (2001): 1396-1397.
56. Psomas G., *et al.* "Synthesis, Characterization and DNA-Binding of the Mononuclear Dioxouranium(VI) Complex with Ciprofloxacin". *Polyhedron* 27.1 (2008): 133-138.
57. Butorov E V. "Influence of L-Lysine Amino Acid on the HIV-1 RNA Replication in Vitro". *Antiviral Chemistry and Chemotherapy* 24.1 (2015): 39-46.
58. Bol S and Bunnik E M. "Lysine Supplementation Is Not Effective for the Prevention or Treatment of Feline Herpesvirus 1 Infection in Cats: A Systematic Review". *BMC Veterinary Research* 11.1 (2015): 284.
59. Loh P C and Oie H K. "Role of Lysine in the Replication of Reovirus". *Journal of Virology* 4.6 (1969): 890-895.
60. Corbau, R., *et al.* "Lersivirine, a Nonnucleoside Reverse Transcriptase Inhibitor with Activity against Drug-Resistant Human Immunodeficiency Virus Type 1". *Antimicrobial Agents and Chemotherapy* 54.10 (2010): 4451-4463.

Assets from publication with us

- Prompt Acknowledgement after receiving the article
- Thorough Double blinded peer review
- Rapid Publication
- Issue of Publication Certificate
- High visibility of your Published work

Website: www.actascientific.com/

Submit Article: www.actascientific.com/submission.php

Email us: editor@actascientific.com

Contact us: +91 9182824667